Check for updates

ChemistrySelect

Research Article
doi.org/10.1002/slct.202401334

Chemistry Europe
European Chemical Societies Publishing

www.chemistryselect.org

Effect of Metal Coordination Environment on the Stability of Zinc Complexes and Their Reactivity with NaSH

Marina Lamberti,*[a] Maria Vittoria Galotto,[a] Ermanno Vasca,[a] Alessandro Landi,[a] Andrea Peluso,[a] and Maria Strianese*[a]

Metal complexes with multidentate ligands are frequently used as model compounds to shed light on the (bio)-inorganic chemistry of H_2S. Zinc complexes bearing salen-type ONNO ligands with different bridging groups are particularly relevant in this respect. Here, we describe the use of zinc complexes with the sulfur-analogues of the ONNO ligands with the S-donors replacing either the neutral nitrogen donors or the anionic oxygen atoms of the classical salen ligands. In addition, we studied a hexadentate cyclic ligand, with four neutral sulfur atoms and two anionic oxygens. Having two coordinative pockets this ligand is able to form a bimetallic zinc complex. We report how the different coordinative environments of the explored ligands influence the stability of the zinc complexes and their abilities to form the related hydrosulfide species.

Introduction

Hydrogen sulfide (H_2S) possesses important signaling and regulatory functions within the human body. With nitric oxide (NO) and carbon monoxide (CO) it belongs to the family of the "*gasotransmitters*".[1–3] Whereas the chemical biology of NO and CO has been well studied, this is much less so for H_2S. Among the cellular targets of H_2S, the transition metals constitute the more common sites of attack as they easily react with the Lewis-base sulfur of H_2S.[4–11] More recent studies revealed signaling pathways involving metalloproteins.[12–16]

In this context, motivated by our aim of clarifying the reactions H_2S is involved in, our studies on the coordination of H_2S to transition metals started a few years ago and focused both on properly tailored low molecular weight metal complexes and on natural metalloproteins.[17–24] Recently we and others focused on the synthesis of fluorescent salen-based zinc complexes.[25–35] It was of interest to establish how the 'hardness/softness' of imine and amine nitrogens (which chelate the zinc centers) of the resulting complexes may affect the HS^- binding.[36] The ligands we explored so far, all have anionic phenolate oxygens and neutral imino or amino nitrogens, two hard donor atoms whose combination reduces the possibility to modulate the electronic features of the metal centre.[37] Inspired by the ubiquity in nature of sulfur-rich metalloproteins and metalloenzymes,[38] we decided to focus on the sulfur-analogues of the classical ONNO-ligands and to investigate how the electronic properties and the Lewis acidity of the metal might affect the propensity to coordinate H_2S/HS^-.

The so-called OSSO-type bis-(phenolato) ligands were initially developed by Okuda and coworkers in the early 2000s and have interesting catalytic applications (e.g. the isotactic polymerization of styrene).[39] Later on, the group of Kol proposed a new straightforward synthetic route for these OSSO-type ligands producing complexes that catalyze the formation of stereo-irregular poly(1-hexene).[40] In more recent years, these OSSO-type bis-(phenolato) ligands have been reported as alternatives to produce active zirconium complexes which catalyze the polymerization of L-lactide and also the reaction of CO_2 with epoxides.[41]

The replacement of nitrogen atoms of the diimine moiety in salen ligands by sulfur atoms recently found successful applications in the cleavage of carbon-sulfur bond chemistry, a process useful in the desulfurization of petroleum, and the aerobic oxidative cleavage of ß-keto-sulfides.[42]

Here we report on the synthesis of three zinc complexes[40,43–45] bearing different sulfur-containing ancillary ligands (Scheme 1) and we explore their interactions with HS^-. In complex **1**, the sulfur atoms substitute the anionic oxygens of the classical salen ligands whereas the imine N-donors remain unaltered resulting in a SNNSZn complex. In complex **2**, sulfur atoms replace the imine nitrogens of the classical salen-type ONNO ligands and thus the anionic oxygen atoms are

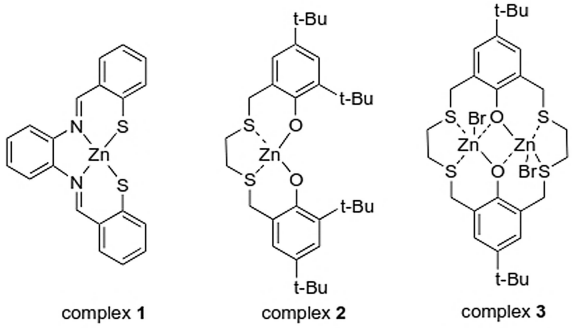

Scheme 1. Structures of the complexes investigated in this work.

[a] *M. Lamberti, M. V. Galotto, E. Vasca, A. Landi, A. Peluso, M. Strianese*
Dipartimento di Chimica e Biologia "Adolfo Zambelli", Università degli Studi di Salerno, Via Giovanni Paolo II, 132, 84084 Fisciano (SA), Italy
E-mail: mlamberti@unisa.it
mstriane@unisa.it

Supporting information for this article is available on the WWW under https://doi.org/10.1002/slct.202401334

© 2024 Wiley-VCH GmbH

paired with neutral thioether groups resulting in a sulfur-bridged OSSOZn complex. For both complexes **1** and **2** the zinc atoms are tetracoordinated. Finally, in complex **3**, we have chosen a hexadentate, bianionic, cyclic ligand which has two coordinative pockets. They can host two metal centers allowing the obtainment of a zinc bimetallic complex.[45] In this case, each zinc atom is pentacoordinate, since, in addition to the coordination with two oxygens and two sulfur atoms of the ligand, it also binds an additional bromide ligand.

As a hard acid, zinc usually forms stronger bonds with first-row donor atoms, such as oxygen and nitrogen, than with second-row atoms, such as sulfur and phosphorus. For example, in complexes bearing SNNS-type ligands[43,44] the S–Zn bonds are longer than the O–Zn bonds in the ONNOZn complexes. In the current contribution, we wonder if a weaker coordination of the ancillary ligand to the zinc, resulting in a higher Lewis acidity of the metal center, could enhance the ability of the complex to "capture" hydrosulfide species. Devices for measuring H_2S uptake are useful for monitoring gas storage and separation and for monitoring desulfurization processes.

Results and Discussion

Complex **1** was obtained via a template synthesis from *ortho*-phenylene-diamine and thiosalicylaldehyde in the presence of triethylamine in acetonitrile.[43] Complex **2** was synthesized by the direct reaction of the ligand precursor $OSSOH_2$ and $ZnEt_2$ in dry benzene. Complex **3** was prepared by reacting the lithium salt of the starting ligand precursor $(OSS)_2H_2$ with 2 equivalents of $ZnBr_2$, by slightly changing a literature procedure[45] (see experimental part for more details). Complexes **1**–**3** were first characterized via high-resolution MALDI Fourier transform ion cyclotron resonance mass spectrometry (HR MALDI-FT-ICR) (Figures S1–S3). The major peaks at 432.97 m/z units for complex **1**, at 593.251 m/z units for complex **2** and at 740.94 m/z units for complex **3** correspond to the monomeric species: no evidence of the formation of dimeric species in solution was found. Next, complexes **1**–**3** were characterized via ^{1}H NMR experiments (see Figures 1 and S5, S6). The ^{1}H NMR spectra of complexes **1**–**3** in DMSO-d_6 demonstrated the formation of the desired complexes as they were in agreement with spectra reported in the literature.[44,45] As for complex **1**, proper attribution of the peaks in the ^{1}H NMR spectrum shown in Figure 1, was obtained by the 2D COSY spectrum (Figure S4).

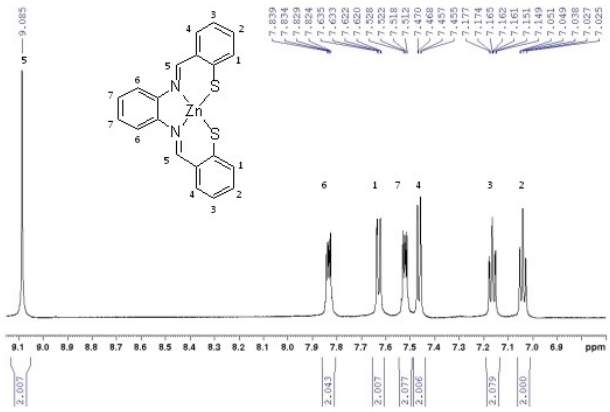

Figure 1. ^{1}H NMR spectrum of complex **1** in DMSO-d_6. [complex **1**] = 3×10^{-2} M.

As for the ^{13}C NMR characterization, we could register the spectrum only for complex **1** (Figure S7) and complex **3** (Figure S8), most likely for the scarce stability in DMSO of complex **2**. Peaks in the ^{13}C NMR spectrum of complex **3** were not very intense due to the very low solubility of the complex in deuterated DMSO.

Complexes **1** and **3** appear robust and stable to air and to trace amounts of water (e.g. their ^{1}H NMR spectra did not change when leaving NMR samples standing for days), whereas complex **2** appeared less stable in solution. Probably, the weaker coordination of sulfurs to the zinc atom, as compared to the chelating nitrogens in the salen-complexes is responsible for the lower stability of this complex. Complexes **1**–**3** were further characterized via IR spectroscopy in KBr (Figures S9–S11); the spectra resemble the literature data.[44,45] After characterization of complexes **1**–**3** we initiated a study to determine if they are able to form stable adducts with HS^-. We first examined the reactions via ^{1}H NMR spectroscopy examining the proton NMR spectra of complexes **1**–**3** after the addition of known amounts of NaSH. As for complex **1**, analysis of ^{1}H NMR spectra before and after addition of 2 equivalents of NaSH indicates that a new species is forming: a shift of the whole peak pattern is observed (see Figure S12). In addition, a high-field resonance (at −2.9 ppm) attributable to the HS^- group bound to the zinc is present, in agreement with other spectra of metal hydrogensulfide complexes.[46–48] However, the integral of the high-field peak is not pointing to the quantitative formation of the binding adduct (see Figure S12): most likely the hydrogensulfide adduct is in equilibrium with the free complex **1**, a phenomenon which could also explain the broadening of the signals in the aromatic region. Thus, we examined the ^{1}H NMR spectrum obtained after addition of 4 equivalents of NaSH to complex **1**. In this case the presence of more than one species is evident. On the other hand, a peak at −2,6 ppm was clearly visible, the integral of which points to the capture of 1 equivalent of HS^- (Figure S13). The formation of different species following the addition of 4 equivalents of NaSH, could be ascribed to the tendency of the complexes of this class to form aggregates in solution,[43,44] a phenomenon which, in this case, could be assisted by the presence of the SH^- coordinated to the zinc centers.

In the case of complex **2**, a shift of the proton pattern is again visible but the high-field resonance is lacking (Figure S14). When H_2S/HS^- interacts with a metal complex, three scenarios are possible: (i) displacement of the metal from the ligand via HS^- mediated precipitation of metal sulfides, (ii) binding of HS^- to the metal center, and (iii) HS^- mediated reduction of the metal center. The last scenario entails redox activity of the metals and can be discarded in our case since zinc is a non-redox metal.

By comparison of the proton NMR spectrum of complex **2** upon treatment with HS^- and that of the free ligand $OSSOH_2$ (Figure S15) we can exclude that the interaction of complex **2**

© 2024 Wiley-VCH GmbH

23656549, 2024, 21, Downloaded from https://chemistry-europe.onlinelibrary.wiley.com/doi/10.1002/slct.202401334 by Universita Di Salerno, Wiley Online Library on [16/09/2024]. See the Terms and Conditions (https://onlinelibrary.wiley.com/terms-and-conditions) on Wiley Online Library for rules of use; OA articles are governed by the applicable Creative Commons License

and HS^- results in the zinc displacement and leaching of the organic ligand. Consequently, the hypothesis that HS^- binds to complex **2** becomes the most probable: the lacking of the high field resonance even upon coordination of HS^- to the zinc center is not new[22,24] and can be explained by the exchange of the Zn-SH signal with the trace amounts of water in deuterated DMSO. Further supporting the latter hypothesis is the disappearance of the H_2O signal at 3.3 ppm which is present, for instance, in the ^{1}H NMR spectrum of complex **2** before adding NaSH (see Figure S5).

Intriguingly, in the case of complex **3**, we observed an increased solubility when NaSH was added: the suspension of the complex in DMSO rapidly turned to a colorless solution. We interpreted this as a first indication that adduct formation occurs. Figure 2 displays the ^{1}H NMR spectrum of complex **3** in the presence of 2 equivalents of HS^-.

The high-field resonance at −2.32 ppm (which integrates to two protons) ascribable to the SH groups bound to the zinc centers is clearly evident. The broadness of the signal could be due to a proton exchange between SH and H_2O (which is present in deuterated DMSO).[34,49] A further indication that a new species is formed when adding HS^- to a DMSO-d_6 solution of complex **3**, is the shift of the signal of the methylene protons of the free complex with respect to that of the HS-reacted species (Figure S16).

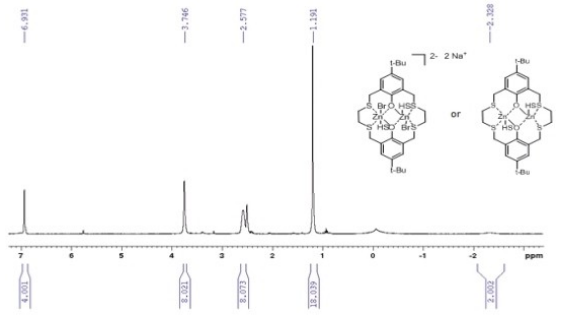

Figure 2. ^{1}H NMR spectrum of complex **3** in DMSO-d_6 after the addition of 2 equivalents of HS^-. [complex **3**] = 8×10^{-3} M; [NaSH] = 0.016 M.

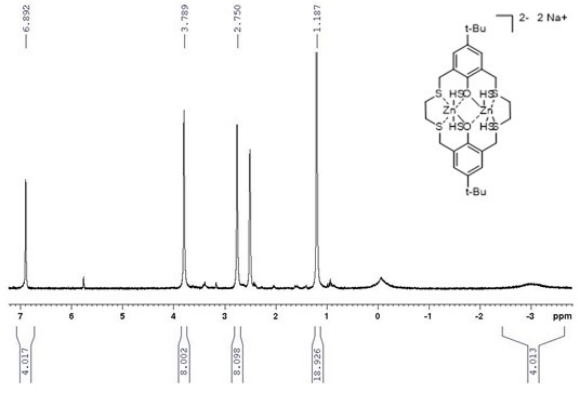

Figure 3. ^{1}H NMR spectrum of complex **3** in DMSO-d_6 after the addition of 4 equivalents of HS^-. [complex **3**] = 8×10^{-3} M; [NaSH] = 0.032 M.

We conclude that two possible species could be formed: either the HS^- can substitute the bromide ligands by furnishing a neutral bimetallic complex in which each zinc atom is still pentacoordinate, or the two HS^- ions may add to the zinc atoms making the zinc hexacoordinate and giving the disodium salt of a bianionic complex.

When adding four equivalents of HS^- to a sample of complex **3**, the ^{1}H NMR spectrum of the reaction mixture exhibits a further change (Figure 3): the high-shielded signal of the HS^- bound to the zinc ions corresponds upon integration to 4 protons and there is a further shift towards high field. Also in this case, the other significant change of the NMR spectrum concerns the signal of the methylene protons bridging the two sulfur atoms.

This finding is consistent with there action proposed in Scheme 2, the species formed is a bi-anionic complex where each zinc is hexacoordinate and the adduct is in the form of the sodium salt.

A ^{1}H NMR spectrum very similar to that shown in Figure 3 was obtained when adding first two equivalents of HS^- to complex **3** in DMSO-d_6 and subsequently two more equivalents.

The ^{13}C NMR spectrum of the complex **3** upon HS^- addition (four equivalents) is displayed in Figure S17. A further confirmation of the formation of the HS^- binding adduct comes from the comparison of the ^{13}C NMR spectra before and after HS^- addition (Figure S8) where a shift of the whole pattern is clearly evident.

In order to gain a better insight into the structures of the complexes under investigation and to have an indication of their possible reactivity with HS^-, we performed a computational analysis with time dependent density functional theory (TD-DFT). Minimum energy geometries of complex **2** and complex **3** and of their HS^- adducts (also considering the possibility of multiple adducts) have been computed both for the ground state and for the first excited singlet states. The computed ground state optimum geometries of HS^- complexes for **2** and **3** are shown in Figure 4.

Complexes **2** and **3** deviate from the square planar nuclear configuration observed for salen analogues,[32,33] with the metal atom in the plane of the ligand (see Figure 5). The formation of the double HS^- adduct for the bimetallic complex **3** is predicted to take place through coordination of HS^- to the Zn atoms and the expulsion of the two Br^- ions ($\Delta E = -1.24$ eV). ΔE is the thermodynamic energy change for the substitution of the Br^- ligands with HS^-, i.e. for the reaction:

$$M{-}Br_n + n\,HS^- \rightarrow M{-}(HS)_n + n\,Br^-$$

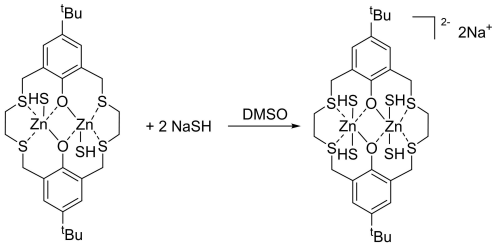

Scheme 2. Species formed upon reaction of complex **3** and HS^-.

© 2024 Wiley-VCH GmbH

23656549, 2024, 21, Downloaded from https://chemistry-europe.onlinelibrary.wiley.com/doi/10.1002/slct.202401334 by Universita Di Salerno, Wiley Online Library on [16/09/2024]. See the Terms and Conditions (https://onlinelibrary.wiley.com/terms-and-conditions) on Wiley Online Library for rules of use; OA articles are governed by the applicable Creative Commons License

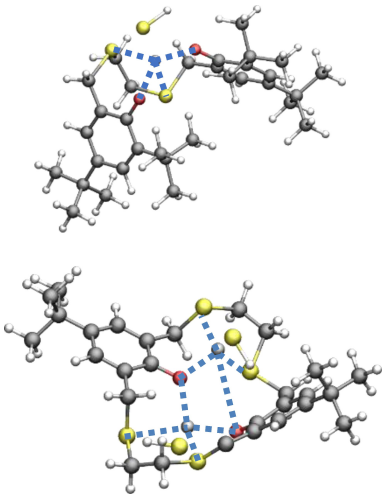

Figure 4. Optimized geometries for the adducts with HS^- of **2** (top) and **3** (bottom).

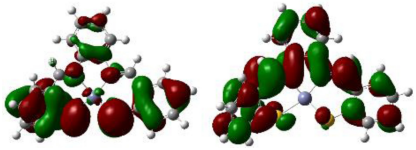

Figure 5. HOMO (left) and LUMO (right) of complex **1**.

However the structure of the bimetallic complex does not change significantly upon the substitution of the Br ligands with HS ligands. When considering the possibility where both HS^- and Br^- are coordinated to the Zn, this adduct is not predicted to be a stable species by DFT.

To gain independent evidence of the reactivity with HS^- of the complexes under investigation, we investigated the reactions *via* UV-Vis and fluorescence spectroscopies. Figure S18 displays the electronic absorption spectra of complexes **1** and **2** before and after the treatment with an excess of HS^-. In case of complex **1** the spectrum exhibits two bands at 334 and 427 nm, which may be attributed to intramolecular π-π* charge transfer bands (see Figure 5 and Table S1).

Upon NaSH addition, the 334 band quenches, whereas the 425 nm band shifts to 432 nm. The titration data could be interpreted assuming the formation of a 1.1 adduct according to the reaction:

$$LM + L' = LML'$$

with $\log K = 4.24 \pm 0.05$ (the uncertainty is 3σ; Figures S19 and S20).[50] In the above equation L is the organic ligand chelating zinc whereas L′ stands for HS^-; K is the association constant (see SI for further details).

As for complex **2**, the UV-vis spectrum does not undergo visible shifts but a quenching of the whole absorption spectrum was registered. Moreover, for complex **2**, we could measure also the absorption spectrum of the free $OSSOH_2$ ligand and exclude that the reaction of this complex with HS^- results into the leaching of the organic ligand.

Figure 6 displays the same experiment with complex **3**, in this case we registered first the spectrum of the free complex, then the spectrum in the presence of 2 equivalents of HS^- and finally the spectrum after the subsequent addition of two more equivalents, to mimic the conditions of the NMR experiments.

The absorption spectrum of complex **3** before HS^- treatment shows bands only in the UV region (ca. 260–320 nm), in accordance with the Ref. [45].

As evident in Figure 6, the UV-vis spectrum of complex **3** experiences a visible change in the presence of 2 equivalents of NaSH and further changes in the presence of 4 equivalents of NaSH, thus indicating formation of two new species and corroborating the hypothesis made on the basis of the NMR experiments. More specifically, upon reaction with HS^-, a bathochromic shift of the lower energy absorption band is observed. Time dependent density functional theory (TD-DFT) calculation for complex **3** predicts the presence of two electronic transitions with similar intensities at λ 320 nm and 285 nm, respectively. The character of the transitions is metal-ligand charge transfer (MLCT); indeed: the LUMO is a non-bonding π MO with significant contributions from the π orbitals of the benzene ring of the ligand, while other orbitals involved in the transitions also involve the Br atoms bound to Zn centers (see the Molecular Orbitals reported in Figure S21).The replacement of bromine anions with HS^- groups leaves the predicted wavelengths of the transitions essentially unchanged, 330 nm and 291 nm, while their relative intensity significantly changes, the latter becoming almost three times more intense than the former, in good agreement with experimental findings. Indeed, the transition at longer wavelength involves molecular orbitals with significant contribution of Br^- and HS^-, being therefore sensitive to HS^- coordination. After the coordination of HS^-, the character of the transition is the same as in the starting Br complex: the LUMO is a nonbonding π MO with significant

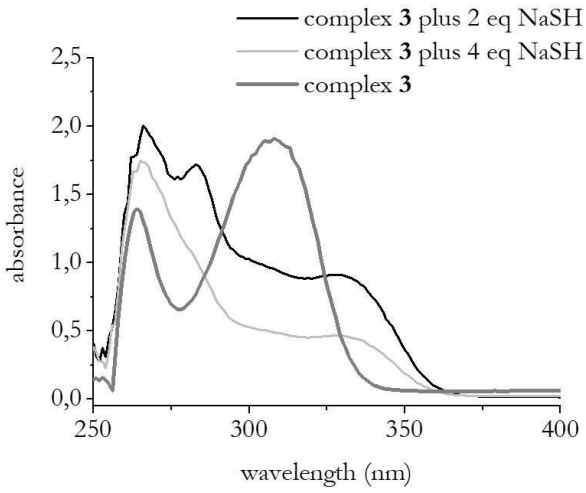

Figure 6. Electronic absorption spectra of complex **3** with and without the addition of NaSH. Spectra were recorded in DMSO at room temperature. [complex **3**] = 10 μM.

© 2024 Wiley-VCH GmbH

23656549, 2024, 21, Downloaded from https://chemistry-europe.onlinelibrary.wiley.com/doi/10.1002/slct.202401334 by Universita Di Salerno, Wiley Online Library on [16/09/2024]. See the Terms and Conditions (https://onlinelibrary.wiley.com/terms-and-conditions) on Wiley Online Library for rules of use; OA articles are governed by the applicable Creative Commons License

contributions from the π orbitals of the benzene ring of the ligand, while other orbitals involved in the transitions also involve the S atoms bound to Zn centers (orbitals not shown since they are identical to the ones shown in Figure S21).

Both the scan and the time trace fluorescence emission spectra indicate a fluorescence intensity change of complex **3** in the presence of NaSH (see Figure S22), thus supporting the formation of a new species.

Conclusions

In this work we synthesized two zinc complexes derived from the S-analogues of the ONNO ligands and a bimetallic zinc complex supported by a hexadentate $(OSS)_2H_2$ ligand (Scheme 1). The possible effects of the different coordinative environments on the zinc hydrosulfide stabilization were investigated. Complexes **1**–**3** were characterized by NMR, MALDI-ToF and UV-vis analyses. Complex **1** was found to be prone to HS^- binding. As for complex **2**, the poor stability of the Zn-SH adduct complicated our characterizations and made this complex ill-suited for our purposes.

Replacing the hard donors in the skeleton of the chelating salen-type ligands with the softer sulfur-based donors resulted in a reduced stability of the complex (as happens for complex **2**) or in a lower selectivity in the reaction with NaSH (as in the case of complex **1**, which forms more than one adduct).

On the other hand, the bimetallic complex **3** with its cyclic ligand, appeared stable also when HS^- was bound. In this case, NMR experiments, corroborated by DFT calculations, point to the formation of a neutral HS^- adduct where the two bromide ligands are substituted by two HS groups, as displayed in Figure 4. The formed species appeared stable overtime and was able to coordinate two additional HS groups. Most likely, the different coordinative environment of the metal centers and the constrained geometry of the cyclic ligand guarantee greater stability of the complex itself and of the adducts that form from it. Electronic effects of the ligand skeleton may impart increased Lewis acidity to the Zn center in complex **3** thus ensuring a stronger bond with HS ions.

We believe the results we report herein provide clear evidence that the coordination sphere surrounding the metal center plays a key role both in the stability of the complex and in the ability of the zinc center to bind HS^-.

We are currently investigating the possible application of complex **3** in the implementation of a device for HS^- uptake.

Materials and Methods

Chemicals used for the synthetic work were obtained from Sigma-Aldrich and were of reagent grade. They were used without further purification. NaSH (Alfa Aesar) in aqueous solution was used as HS^- source to the end concentration specified in the figure captions. Synthesis of ligand $OSSOH_2$ was achieved by following literature procedures.[40] Ligand $(OSS)_2H_2$ was prepared by modification of a procedure reported in the literature.[45] Complex **1** was obtained by a procedure reported in the Refs. [43,44].

General

HR MALDI and ESI mass spectra were recorded using a Bruker solariX XR Fourier transform ion cyclotron resonance (FT-ICR) mass spectrometer (Bruker Daltonik GmbH, Bremen, Germany) equipped with a 7 T refrigerated actively-shielded superconducting magnet (Bruker Biospin, Wissembourg, France). The samples were ionized in positive ion mode using either the MALDI ion or the ESI ion source. The mass range was set to *m/z* 150–2000. The laser power was 15 % and 15 laser shots were used for each scan. Mass spectra were calibrated externally using a mix of peptide clusters in MALDI ionization positive ion mode. As for the ESI mass spectra, they were calibrated externally using a NaTFA solution in negative ion mode. A linear calibration was applied.

NMR spectra were recorded on a Bruker AVANCE 400 NMR instrument (^{1}H NMR, 400.13 MHz; ^{13}C NMR, 100.62 MHz) or on a 600 MHz spectrometer [600 (^{1}H NMR) and 150 MHz (^{13}C NMR)] using 5 mm o.d. NMR tubes. The chemical shifts were reported in δ (ppm) referenced to SiMe4. Typically, 5 mg of the complex in 0.5 mL of the solvent were used for each experiment. MilliQ water and is the water filtered with a Millipore filter apparatus.

Synthesis and Characterization of Complex 1

Synthesis of complex **1** was achieved by following a template synthesis reported in the literature.[43,44] To a CH_3CN solution of 2,4-di-tert-butyl-thiosalicyladehyde[43] (1.15 g, 8.3 mmol), $Zn(OAc)_2 \cdot 2H_2O$ (0.55 g, 2.5 mmol) and triethylamine (2 ml, 15 mmol) in MeOH (5 ml) were slowly added. The reaction flask was left under stirring in the dark and a solution of orto-phenilendiamine (0.27 g, 2.5 mmol) in MeOH (5 ml) was added dropwise at room temperature. The resulting red solution was left under stirring for 17 h in the dark. A red precipitate was recovered by filtration, washed with cold methanol and dried under vacuum (0.465 g, yield: 45 %). IR (cm^{-1}, KBr, selected): 1615, 1578, 1450, 1384, 1184, 1076, 739. Anal. Calcd for C20H14N2S2Zn: C, 58.32; H, 3.43; N, 6.80; S, 15.57. Found: C, 58.23; H, 3.62; N, 6.98; S, 15.01. MS (MALDI FT-ICR MeOH): m/z (%) calculated: 410.996 experimental: 410.996 [complex 1 + H]$^+$. ^{1}H-NMR (600 MHz, DMSO-d_6): δ = 9.08 (s, 2H, N=CH), 7.82 (m, 2H, ArH), 7,63 (d, 2H, ArH), 7.51 (m, 2H, ArH),7.45 (d, 2H, ArH), 7.16 (t, 2 H, ArH), 7.02 (t, 2H, ArH).

Synthesis and Characterization of Ligand $OSSOH_2$[40]

Under a nitrogen atmosphere, a solution of 1,2-ethanedithiol (0.22 ml, 4.39 mmol) and triethylamine (0.70 ml, 5.0 mmol) was added dropwise to a solution of 2-bromomethyl-4,6-di-tert-butyl-phenol (1.50 g, 5.0 mmol) in THF dry (5.83 ml). A white solid formed immediately. The reaction mixture was left under stirring and in the dark at room temperature for 24 h. Then a white powder was filtered off. The THF solution was dried under vacuum and a yellow solid formed. Dichloromethane (10.0 mL) was then used to dissolve the yellow powder, the resulting solution was extracted with H_2O (3×1 mL) and then dried over Na2SO4.At this point the colorless solution was dried under vacuum yielding a yellow solid which was washed with cold methanol and dried again. A white solid was obtained (1.1 g, yield: 47 %). ^{1}H-NMR (400 MHz, C_6D_6): δ = 7.45 (d, 2H, Ar), 6.81 (d, 2H, Ar), 6.70 (s, 2H, OH), 3.33 (s, 4H,CH_2), 2.14 (s, 4H, CH_2), 1.60 (s, 18H, t-Bu), 1.27 (s, 18H, t-Bu), ppm.

Synthesis and Characterization of Complex 2

Under inert atmosphere, a benzene solution of ligand $OSSOH_2$ (153.0 mg, 0.29 mmol) was added dropwise to a solution of Et_2Zn (35.7 mg, 0.29 mmol) in dry benzene. The resulting suspension was

© 2024 Wiley-VCH GmbH

23656549, 2024, 21, Downloaded from https://chemistry-europe.onlinelibrary.wiley.com/doi/10.1002/slct.202401334 by Universita Di Salerno, Wiley Online Library on [16/09/2024]. See the Terms and Conditions (https://onlinelibrary.wiley.com/terms-and-conditions) on Wiley Online Library for rules of use; OA articles are governed by the applicable Creative Commons License

left under stirring and at room temperature for 3 h. A white powder was recovered by removing benzene under vacuum (106.5 mg, yield: 62%). IR (cm^{-1}, KBr, selected): 2954, 1628, 1478, 1244, 1111. Anal. Calcd for C32H48O2S2Zn: C, 64.68; H, 8.14; S, 10.79. Found: C, 64.03; H, 8.62; S, 10.01. MS (MALDI FT-ICR MeOH): m/z (%) calculated: 593.245 experimental: 593.251 [complex 2+H]$^+$. ^{1}H-NMR (400 MHz, DMSO-d_6): $\delta = 7.00$ (s, 1H, Ph–H), 6.85 (s, 1H, Ph–H), 3.70 (s, 2H, Ph-CH_2), 2.76 (s, 2H, CH_2-S), 1.35 (s, 9H, t-Bu), 1.18 (s, 9H, t-Bu) ppm.

Synthesis and Characterization of Ligand $(OSS)_2H_2$

This ligand was obtained by a modification of the procedure in reference.[45] To a THF (15 ml) solution of 2,6-dibromomethyl-4-tert-butyl-phenol[1,2](1.00 g, 2.98 mmol) was added 1,2-ethanedithiol (0.25 ml, 2.98 mmol). The reaction mixture was refluxed for 15 min and then cooled down at 0 °C. Triethylamine (0.83 ml, 6.00 mmol) was added dropwise. At this point the reaction mixture was left under stirring at room temperature for 30 min then at 45 °C for further 24 h. By filtration a white powder was recovered and then discarded, the remaining solution was dried under vacuum yielding an oil which was then dissolved in diethyl ether (30 mL). A white precipitate was recovered by filtration and dried under vacuum (235.5 mg, yield: 29%). ^{1}H-NMR (300 MHz, $CDCl_3$): $\delta = 7.06$ (s, 2H, Ar), 3.78 (s, 4H, Ph-CH_2), 2.68 (s, 4H, CH_2), 1.26 (s, 9H, t-Bu) ppm.

Synthesis and Characterization of Complex 3

Complex **3** was prepared by a modification of a literature procedure.[45] Under nitrogen, ligand $(OSS)_2H_2$ (0.19 g, 0.35 mmol) was dissolved in dry THF (10 ml) and BuLi (2.5 M, 0.32 ml, 0.81 mmol) was added dropwise at 0 °C. The reaction mixture was left under stirring for 30 min. Then the mixture was allowed to reach room temperature and $ZnBr_2$ (0.18 g, 0.81 mmol) was added. THF dry (10 mL) was added via cannula and left under stirring for 48 h. A yellow oil was obtained by evaporating the solvent under vacuum. A white solid was recovered by washing the oil with CH_2Cl_2 (20 mg, yield: 7%). IR (cm^{-1}, KBr, selected): 2957, 1624, 1479, 1272, 1103. Anal. Calcd for C28H38Br2O2S4Zn2: C, 40.74; H, 4.64; S, 15.54. Found: C, 40.03; H, 4.92; S, 15.01. MS (MALDI FT-ICR $CHCl_3$): m/z (%) calculated: 740.948 experimental: 740.951 [complex 3-Br]$^+$. ^{1}H-NMR (600 MHz, DMSO-d_6): $\delta = 6.89$ (s, 4 H, Ar), 3.79 (s, 8H, Ph-CH_2), 2.74 (s, 8H, CH_2), 1.18 (s, 18H, t-Bu) ppm.

Absorbance and Fluorescence Measurements

Absorption spectra were recorded on a Cary-50 Spectrophotometer, using a 1 cm quartz cuvette (Hellma Benelux bv, Rijswijk, Netherlands) and a slit-width equivalent to a bandwidth of 5 nm. Fluorescence spectra were measured on a Cary Eclipse Spectrophotometer in a 10×10 mm^2 airtight quartz fluorescence cuvette (Hellma Benelux bv, Rijswijk, Netherlands) with an emission band-pass of 10 nm and an excitation band-pass of 5 nm. Both absorption and fluorescence measurements were performed in DMSO solutions at 25 °C. Fluorescence emission spectra were registered by exciting the samples at a specific wavelength (as stated in the figure caption).

NMR Characterization of the Complexes 1–3 Upon Addition of HS^-

The NMR tube was charged with the free complex solutions in DMSO-$d_6$then NaSH solid or in solution (to the end concentrations specified in the figure captions) was added and the spectra registered.

Computational Details

All electronic computations have been carried out at the density functional level of theory using the range separated hybrid functional CAM-B3LYP[51,52] with TZVP basis set as implemented in the Gaussian package (G16).[53] Effects due to solvent polarization were included by the polarizable continuum model (PCM).[54,55] The solvent is the same used experimentally, i.e. DMSO; we used 30 roots in TDDFT calculations.

Acknowledgements

Authors wish to thank Dr. Patrizia Oliva and Dr. Patrizia Iannece from Università degli Studi di Salerno for their technical assistance.

Conflict of Interests

The authors declare no conflict of interest.

Data Availability Statement

The data that support the findings of this study are available in the supplementary material of this article.

Keywords: coordination chemistry · H_2S/HS^- · sulfur-containing ligands · zinc complexes

[1] C. Q. Chen, H. Xin, Y. Z. Zhu, *Acta Pharmacol. Sin.* **2007**, *28*, 1709–1716.
[2] L. Li, P. K. Moore, *Biochem. Soc. Trans.* **2007**, *35*, 1138–1141.
[3] L. Li, P. K. Moore, *Trends Pharmacol. Sci.* **2008**, *29*, 84–90.
[4] M. D. Hartle, S. K. Sommer, S. R. Dietrich, M. D. Pluth, *Inorg. Chem.* **2014**, *53*, 7800–7802.
[5] M. D. Hartle, J. S. Prell, M. D. Pluth, *Dalton Trans.* **2016**, *45*, 4843–4853.
[6] M. D. Hartle, M. R. Tillotson, J. S. Prell, M. D. Pluth, *J. Inorg. Biochem.* **2017**, *173*, 152–157.
[7] M. D. Pluth, Z. J. Tonzetich, *Chem. Soc. Rev.* **2020**, *49*, 4070–4134.
[8] Z. J. Tonzetich, H_2S and Bioinorganic metal complexes in *Hydrogen Sulfide* **2022**, 103–141.
[9] D. C. Mudalige, E. S. Ma, S. J. Rettig, B. R. James, W. R. Cullen, *Inorg. Chem.* **1997**, *36* 5426–&.
[10] J. Pleus, H. Waden, W. Saak, D. Haase, S. Pohl, *J. Chem. Soc. Dalton Trans.* **1999**, *15*, 2601–2610.
[11] H. M. Smith, M. D. Pluth, *JACS Au* **2023**, *3*, 2677–2691.
[12] M. R. Filipovic, J. Zivanovic, B. Alvarez, R. Banerjee, *Chem. Rev.* **2018**, *118*, 1253–1337.
[13] H. Kimura, Signaling by Hydrogen Sulfide (H_2S) and Polysulfildes (H_2S_n) and the Interaction with other signaling pathways in *Hydrogen Sulfide* **2022**, pp. 27–47.
[14] H. Kimura, *Antiox. Redox. Signal* **2014**, *22*, 362–376.
[15] G. K. Kolluru, X. Shen, S. C. Bir, C. G. Kevil, *Nitric Oxide* **2013**, *35*, 5–20.
[16] R. Banerjee, *Antiox. Redox. Signal* **2011**, *15*, 339–341.
[17] M. Strianese, A. Varriale, M. Staiano, C. Pellecchia, S. D'Auria, *Nanoscale* **2011**, *3*, 298–302.
[18] M. Strianese, S. Milione, V. Bertolasi, C. Pellecchia, A. Grassi, *Inorg. Chem.* **2011**, *50*, 900–910.
[19] M. Strianese, G. J. Palm, S. Milione, O. Kuhl, W. Hinrichs, C. Pellecchia, *Inorg. Chem* **2012**, *51*, 11220–11222.

© 2024 Wiley-VCH GmbH

23656549, 2024, 21, Downloaded from https://chemistry-europe.onlinelibrary.wiley.com/doi/10.1002/slct.202401334 by Universita Di Salerno, Wiley Online Library on [16/09/2024]. See the Terms and Conditions (https://onlinelibrary.wiley.com/terms-and-conditions) on Wiley Online Library for rules of use; OA articles are governed by the applicable Creative Commons License

[20] M. Strianese, S. Mirra, V. Bertolasi, S. Milione, C. Pellecchia, *New J. Chem.* **2015**, *39*, 4093–4099.
[21] M. Strianese, G. Zauner, A. W. Tepper, L. Bubacco, E. Breukink, T. J. Aartsma, G. W. Canters, L. C. Tabares, *Anal. Biochem.* **2009**, *385*, 242–248.
[22] M. Strianese, S. Mirra, M. Lamberti, C. Pellecchia, *Inorg. Chim. Acta* **2017**, *466*, 426–431.
[23] M. Strianese, G. J. Palm, D. Kohlhause, L. A. Ndamba, L. C. Tabares, C. Pellecchia, *Eur. J. Inorg. Chem.* **2019**, *2019*, 885–891.
[24] M. Strianese, S. Brenna, G. A. Ardizzoia, D. Guarnieri, M. Lamberti, I. D'Auria, C. Pellecchia, *Dalton Trans.* **2021**, *50*, 17075–17085.
[25] G. Consiglio, I. P. Oliveri, S. Failla, S. Di Bella, *Molecules* **2019**, *24*, 2514.
[26] G. Consiglio, S. Failla, I. P. Oliveri, R. Purrello, S. Di Bella, *Dalton Trans.* **2009**, *47*, 10426–10428.
[27] G. Consiglio, S. Failla, P. Finocchiaro, I. P. Oliveri, R. Purrello, S. Di Bella, *Inorg. Chem.* **2010**, *49*, 5134–5142.
[28] G. Consiglio, S. Failla, P. Finocchiaro, I. P. Oliveri, S. D. Bella, *Dalton Trans.* **2012**, *41*, 387–395.
[29] G. Consiglio, I. P. Oliveri, S. Failla, S. Di Bella, *Molecules* **2019**, *24*, 2514.
[30] S. Di Bella, *Dalton Trans.* **2021**, *50*, 6050–6063.
[31] D. Xie, J. Jing, Y. B. Cai, J. Tang, J. J. Chen, J. L. Zhang, *Chem. Sci.* **2014**, *5*, 2318–2327.
[32] M. Strianese, G. Ferrara, V. Vykhovanets, N. Blal, D. Guarnieri, A. Landi, M. Lamberti, A. Peluso, C. Pellecchia, *Sensors* **2023**, *23*, 2023.
[33] M. Strianese, D. Guarnieri, M. Lamberti, A. Landi, A. Peluso, C. Pellecchia, *Inorg. Chem.* **2020**, *59*, 15977–15986.
[34] M. Strianese, M. Lamberti, C. Pellecchia, *Dalton Trans.* **2018**, *47*, 17392–17400.
[35] M. Strianese, M. Lamberti, A. Persico, C. Pellecchia, *Inorg. Chim. Acta* **2019**, *501*, 119235.
[36] M. Strianese, G. J. D'Auria, M. Lamberti, A. Landi, A. Peluso, A. Varriale, S. D'Auria, C. Pellecchia, *Dalton Trans.* **2023**, *52*, 1357–1365.
[37] V. Paradiso, V. Capaccio, D. H. Lamparelli, C. Capacchione, *Coord. Chem. Rev.* **2021**, *429*, 213644.
[38] M. Gennari, C. Duboc, *Acc. Chem. Res.* **2020**, *53*, 2753–2761.
[39] C. Capacchione, A. Proto, H. Ebeling, R. Mülhaupt, K. Möller, T. P. Spaniol, J. Okuda, *J. Am. Chem. Soc.* **2003**, *125*, 4964–4965.
[40] A. Cohen, A. Yeori, I. Goldberg, M. Kol, *Inorg. Chem.* **2007**, *46*, 8114–8116.
[41] V. Paradiso, V. Capaccio, D. H. Lamparelli, C. Capacchione, *Catalysts* **2020**, *10*, 825.
[42] J. Bag, S. Barman, B. K. Maiti, K. Pal, *Eur. J. Inorg. Chem.* **2022**, *2022*, e202101107.
[43] P. Stenson, A. Board, A. Marin-Becerra, A. Blake, E. Davies, C. Wilson, J. McMaster, M. Schröder, *Chem. A Eur. J.* **2008**, *14*, 2564–2576.
[44] N. Kumar, A. K. Asatkar, S. Panda, S. S. Zade, *Polyhedron* **2016**, *117*, 718–728.
[45] J. Chen, X. Wu, H. Ding, N. Liu, B. Liu, L. He, *ACS Sustain. Chem. Eng.* **2021**, *9*, 16210–16219.
[46] M. Rombach, H. Vahrenkamp, *Inorg. Chem.* **2001**, *40*, 6144–6150.
[47] E. Galardon, A. Tomas, M. Selkti, P. Roussel, I. Artaud, *Inorg. Chem.* **2009**, *48*, 5921–5927.
[48] D. J. Meininger, M. Chee-Garza, H. D. Arman, Z. J. Tonzetich, *Inorg. Chem.* **2016**, *55*, 2421–2426.
[49] M. Strianese, M. Lamberti, C. Pellecchia, *Dalton Trans.* **2017**, *46*, 1872–1877.
[50] P. Gans, A. Sabatini, A. Vacca, *Talanta* **1996**, *43*, 1739–1753.
[51] A. Velardo, R. Borrelli, A. Capobianco, A. Landi, A. Peluso, *J. Phys. Chem. C* **2019**, *123*, 14173–14179.
[52] T. Yanai, D. P. Tew, N. C. Handy, *Chem. Phys. Lett.* **2004**, *393*, 51–57.
[53] M. J. Frisch, G. W. Trucks, H. B. Schelegel, et al., *Gaussian 09, revision D.01*, Gaussian, Wallingford **2009**. Ref Type: Computer Program.
[54] S. Miertus, E. Scrocco, J. Tomasi, *Chem. Phys.* **1981**, *55*, 117–129.
[55] E. Parisi, A. Landi, S. Fusco, C. Manfredi, A. Peluso, S. Wahler, T. M. Klapötke, R. Centore, *Inorg. Chem.* **2021**, *60*, 16213–16222.

Manuscript received: April 11, 2024

© 2024 Wiley-VCH GmbH

23656549, 2024, 21, Downloaded from https://chemistry-europe.onlinelibrary.wiley.com/doi/10.1002/slct.202401334 by Universita Di Salerno, Wiley Online Library on [16/09/2024]. See the Terms and Conditions (https://onlinelibrary.wiley.com/terms-and-conditions) on Wiley Online Library for rules of use; OA articles are governed by the applicable Creative Commons License